ELSEVIER

Journal of Chromatography A, 830 (1999) 439–451

JOURNAL OF CHROMATOGRAPHY A

Low-molecular-mass anion screening for forensic environmental analyses by capillary zone electrophoresis with indirect UV detection[1]

X. Xu, P.C.A.M. de Bruyn, J.A. de Koeijer, H. Logtenberg*

Ministry of Justice, Forensic Science Laboratory, Volmerlaan 17, 2288 GD Rijswijk, The Netherlands

Received 3 February 1998; received in revised form 13 October 1998; accepted 21 October 1998

Abstract

A method for low-molecular-mass anion screening is described using a buffer composed of 5-sulfosalicylate (SS) as a visualizing ion, hexadimethrine bromide as an electroosmotic flow modifier and Tris as a pH buffer component, at pH 8.6. All ions with effective mobility higher than $26 \cdot 10^{-9}$ m^2 s^{-1} V^{-1} can be separated within 7.5 min under −30 kV. By using the moderately mobile SS ($54 \cdot 10^{-9}$ m^2 s^{-1} V^{-1}), not only the sensitivity of the detection is improved due to its high UV absorptivity, but also a smaller overall overloading effect is achieved. Meanwhile, the resolution of the high mobility ions, which is normally critical, remains almost the same as compared to a chromate buffer. With an electrokinetic injection, the limit of detection (LOD) of the common ions is 2–13 n*M* and the detection range is linear up to 0.5–3 μ*M*. With a hydrostatic injection the LOD is 0.15–1 μ*M* and the detection range is linear up to 25–200 μ*M*. The identification of ions is performed by comparing the mobility of the ions with that of standards, taking the apparent and effective mobility of HCO_3^-, which is normally present in the sample solution, as a reference.

Keywords: Buffer composition; Organic acids; Inorganic anions; Sulfosalicylic acid

1. Introduction

The determination of low-molecular-mass ions is of interest for both environmental and forensic applications and is commonly performed by ion chromatography (IC), which has been used routinely for this purpose for many years. With the emerging of the novel separation technique capillary electrophoresis (CE) [1–6], it is rapidly expanding to the area covered by IC. The separation in CE is based on the mobility difference in the presence of electroosmotic flow (EOF). High efficiency, separation speed and low cost are the major advantages of this new technique.

Since low-molecular-mass ions commonly lack suitable detection properties, indirect detection is normally applied for CE analysis. Applications using UV absorbance [7–9], fluorescence [10,11], and electrochemical detection [12] are reported. As a UV detector is available for all commercial CE instruments, and a UV absorbing ion with suitable optical and electrophoretic properties is often easy to find,

*Corresponding author. Fax: +31-70-413-5454.

[1]Presented at the 10th International Symposium on High Performance Capillary Electrophoresis, Orlando, FL, 31 January–5 February 1998.

0021-9673/99/$ – see front matter
PII: S0021-9673(98)00889-9

UV is commonly the choice for indirect detection schemes in CE.

In conventional CE, the EOF is against the migration direction of the anions. Many anions with high mobility migrate faster than EOF and hence can not reach the detector. Therefore, the EOF is normally reversed to coincide with the anion migration by adding an EOF modifier to the buffer. This modifier is often a cationic surfactant.

A serious problem when using indirect detection in CE is the presence of a concentration overloading effect [13,14]. This effect causes broad, triangular peaks when the effective or ionic mobility of an analyte ion differs from that of the co-ion in the buffer and, hence, impairs the separation and resolution. The larger the mobility difference, the stronger the effect. The rule that is often used to minimize this effect is known as the (effective) mobility match rule [2,8], which states that a symmetric and narrow peak will be obtained if the (effective) ionic mobility of the co-ion matches that of the ion of interest.

Although tremendous work has been done on the separation and detection of low-molecular-mass ions, there are only a few methods dedicated to anion screening. As the range of the ion mobility is so wide, overloading is inevitable. A buffer containing multiple co-ions with different mobility was considered to be a good solution to overcome an overloading effect [15,16]. However, the system peaks and the strange peak behavior of the analyte appearing at some position between the mobilities of the two co-ions limits the use of such a buffer system in indirect detection.

So far the most successful buffer for anion screening uses chromate as a visualizing ion and a patented solution as an EOF modifier [17,18]. However, chromate may lead to a large overloading for the low mobility ions due to its high mobility and can cause severe oxidation of some ions, e.g. sulfur [19]. Another visualizing ion benzenetetracarboxylic acid or pyromellitic acid with a slightly lower mobility than that of chromate was also successfully used and a good separation was achieved for the high mobility inorganic anions [19,20]. However, the interaction between the visualizing ion and the EOF modifier is probably too strong, resulting in an insufficient EOF rate for an ion screening. Other moderate or low mobility visualizing ions may improve the peak shape of the analytes with close or lower mobility but will normally worsen the separation for the ions with a high mobility.

In this paper, a buffer is used, which reduces the overall overloading, while also giving a generally good separation and high sensitivity for a low-molecular-mass anion screening. This implies the use of a visualizing ion with moderate mobility and a high absorption extinction coefficient, a good separation for both common low and high mobility ions and a reasonably fast EOF.

2. Experimental

2.1. Apparatus

A Beckman P/ACE 5500 capillary electrophoresis system (Beckman Instruments, Fullerton, CA, USA) was used. The amount of buffer at both the inlet and the outlet of the capillary was 4 ml. The polyimide-coated fused-silica capillary of 50 μm I.D.×375 μm O.D. was obtained from Polymicro Technologies (Phoenix, AZ, USA). The total length of the capillary was 0.77 m and the length to the detector was 0.70 m. The window of the on-column detector cell was created by burning off a small section (ca. 4 mm) of the polyimide coating, after which the excess residue was wiped off with methanol. The detection was performed with a diode array detector at 210 nm with a band width of 20 nm. The electropherogram at each wavelength was recorded and evaluated with Beckman P/ACE station software (Version 1.0).

2.2. Chemicals and reagents

5-Sulfosalicylic acid (SSA) dihydrate extra pure as purchased from Merck (Darmstadt, Germany), Tris [α,α,α-Tris-(hydroxymethyl)methylamine] from Aldrich-Chemie (Steinheim, Germany), chromium(VI) oxide, 99+% from Acros Organics (Geel, Belgium), hexadimethrine bromide (HDB) from Sigma (St. Louis, MO, USA). All other chemicals used for the preparation of standard ion mixtures were of analytical-reagent grade. Freshly prepared deionized water (18.2 MΩ) was used for the preparation of all solutions. Standard solutions of ion mixtures were

prepared from a freshly prepared solution of sulfite and from individual standard stock solutions of 15 m*M* in water stored at 2°C for other ions.

The separation solution was composed of 3.0 m*M* SSA and 21 m*M* Tris (pH 8.6). The flushing solution (0.001% HDB) was prepared by adding 16 μl of a 0.25% HDB aqueous solution to 4 ml of the separation solution. Both solutions were filtered before use with a Millex-VV syringe filter of 0.1 μm pore size (Product No. SLVV 025 LS; Millipore, Bedford, MA, USA).

2.3. Procedures

A new capillary was first flushed with 0.1 *M* sodium hydroxide solution for 20 min, followed by water for 10 min and finally with the flushing solution for 10 min. The latter solution is kept in the capillary overnight. Each sample was introduced into the capillary by applying a pressure of 70 mbar (0.5 p.s.i.) for 22 s or a voltage of −2 kV for 16 s. The components of the injection solution were separated with the separation solution at −30 kV (5.1 μA) for 7.5 min. The capillary was maintained at constant temperature (30°C). Separated components were monitored at 210 nm. The capillary was flushed backwards between runs with the separation solution for 0.5 min, then forwards with the flushing solution for 1.0 min and finally forwards with the separation solution for 1.5 min.

3. Results and discussion

An indirect detection method was developed for a low-molecular-mass anion screening. The method was optimized to obtain a smaller overall overloading effect, a high detection sensitivity and a good separation for the common anions. The separation solution or buffer consists of 3 m*M* SSA and 21 m*M* Tris. The solution used only for flushing the capillary between electrophoretic runs is prepared by adding the EOF modifier HDB to the SSA–Tris buffer. The electropherograms of the standard mixtures obtained by different injection methods are shown in Fig. 1 (high concentrations) and Fig. 2 (low concentrations). The electropherograms of the dilution water are also given in Fig. 2. The corresponding effective mobilities of the anions are listed in Table 1. This method is evaluated as follows.

3.1. Reduction of the concentration overloading effect

Theoretically, according to the mobility match rules, one way to decrease the effect of concentration overloading for the separation of ions with a wide mobility range is to choose a co-ion with a mobility located near the middle of the mobility range of interest. Visualizing ions with a high mobility, such as chromate [17] and pyromellitate [19,20], were used as a buffer co-ion, in order to obtain sharp peaks and a better separation for the common ions with a high mobility (near $75 \cdot 10^{-9}$ m^2 s^{-1} V^{-1}) such as $S_2O_3^{2-}$, Br^-, Cl^-, SO_4^{2-}, NO_2^-, NO_3^- etc. However, ions with (low) mobilities (around $30 \cdot 10^{-9}$ m^2 s^{-1} V^{-1}) far from that of the co-ion will have a large overloading effect, leading to broad triangular peaks and a poor separation efficiency. Although the peak shape and separation efficiency of analyte ions with moderate or low mobility will be improved by using a co-ion with a mobility in those ranges, the separation of the high mobility ions is then normally largely impaired. This is because those co-ions normally lack the required interaction with other components in the buffer for the separation. In the present method the doubly-charged 5-sulfosalicylate (SS) with its mobility matching formate ($53.65 \cdot 10^{-9}$ m^2 s^{-1} V^{-1}) is chosen as a visualizing ion, not only because it has a much higher UV absorbance and a desired mobility to obtain a smaller overall overloading effect but also because the resolution of the high mobility ions remains almost the same as with the chromate buffer.

3.2. Optimization of the separation

The mutual interaction between analytes and buffer components has a significant influence on the separation of ions, especially on multiply-charged ions. The type and concentration of the buffer components can be manipulated to achieve the desired separation.

A fast reversed EOF is preferred for an ion screening. An EOF modifier plays an important role in reversing the EOF, as well as in the separation.

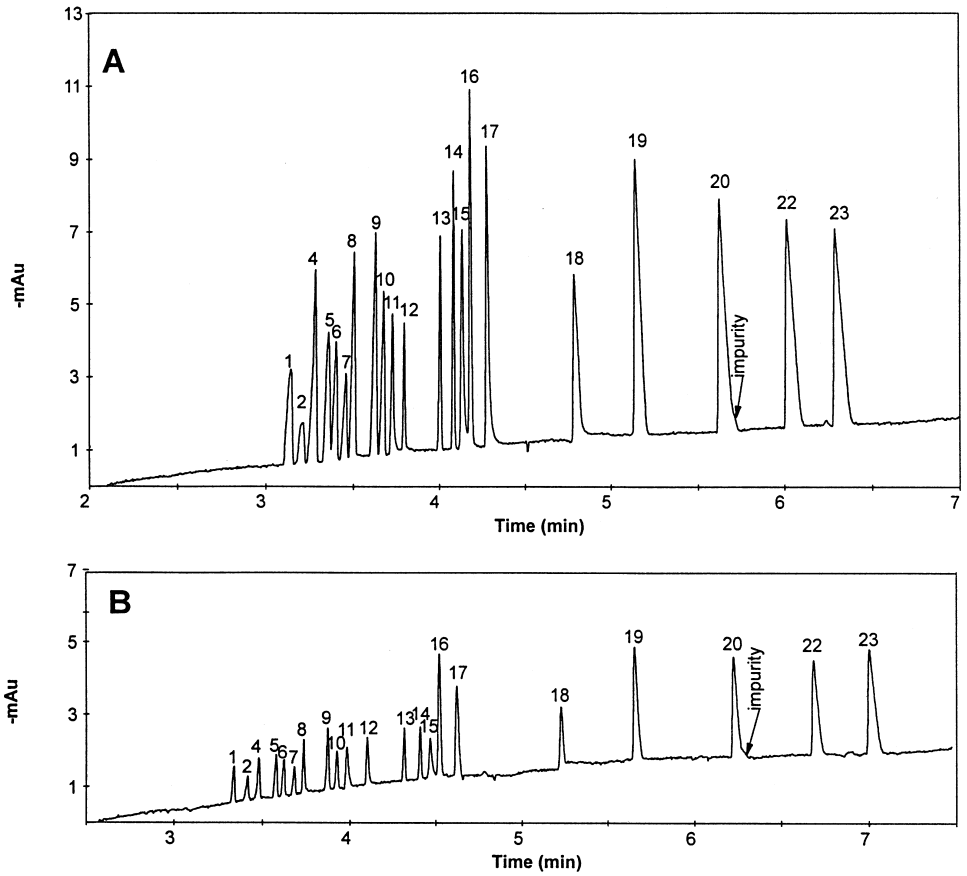

Fig. 1. Separation of the standard ion mixture by: (A) electrokinetic injection at −2 kV for 16 s and (B) pressure injection at 70 mbar (0.5 p.s.i.) for 22 s. The maximum detector photon counts at 254 nm is 8500. Peaks identities (μ*M*, ppm): 1=thiosulfate (5, 0.45); 2=bromide (5, 0.40); 4=chloride (5, 0.18); sulfate (3, 0.29); 6=nitrite (10, 0.46); 7=nitrate (10, 0.62); 8=oxalate (5, 0.53); 9=perchlorate (10, 1.0); 10=thiocyanate (10, 0.58); 11=sulfite (5, 0.40); 12=citrate (5, 0.96); 13=malate (5, 0.57); 14=tartarate (5, 0.74); 15=fluoride (10, 0.19); 16=formate (10, 0.45); 17=hydrogenphosphate (10, 0.95); 18=hydrogencarbonate (17, 1.02); 19=acetate (20, 1.18); 20=propionate (20, 1.46); 22=butyrate (20, 1.74); 23=valerate (20, 2.04). The impurity is a degradation product of the mixture. Other conditions: see Section 2.

Some of EOF-reversing reagents are very effective but may precipitate with multiply charged anions in the buffer or cause a poor separation of the common ions. HDB is found to be one of a few surfactants which are effective as well as of ''non-precipitation'' with many visualizing ions in a wide pH range [20]. A higher concentration of the cationic surfactant in the buffer results not only in a higher reversed EOF but also in a slightly decreased mobility of the analytes with multiple-charges. With HDB being present in the buffer, all multiply-charged ions shift in the low mobility direction and impair the resolution of e.g. $S_2O_3^{2-}/Br^-$, SO_4^{2-}/NO_2^-, tartarate/F^-. To avoid this, in practice, HDB is only added to the flushing buffer to coat the capillary dynamically between electrophoretic runs. The adsorption of HDB to the capillary wall is so strong that the reversed EOF changes only slightly after tens of minutes of electrophoresis with a HDB-free solution.

The counter-ion (also cation) in the buffer has a similar effect as the cation surfactant on the analyte ions. The magnitude of the effect is dependent on the concentration and type (charge, length, size, active points etc.) of the ion. For example, NH_4^+ has less

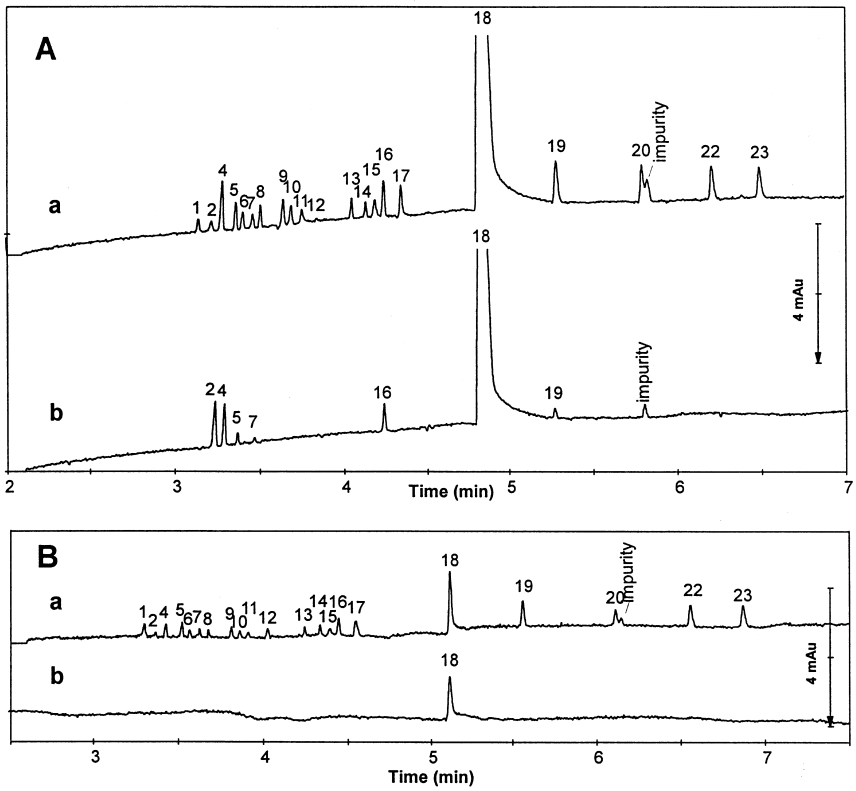

Fig. 2. Electropherograms of: (a) standard ion mixtures and (b) corresponding deionized water used for dilution, by using: (A) electrokinetic and (B) hydrostatic injection. The LODs in Table 2 were calculated from data collected from A,a and B,a. Other conditions are as in Fig. 1.

effect than Tris. The concentration of the counter-ion is mainly dependent on that of the co-ion in the buffer.

The visualizing- or co-ion in the buffer is an anion. It interacts with cations in the buffer and partly offsets their interaction with the analytes. Also the concentration, and particularly the type of co-ion, has an influence on the separation. Among the tested doubly-charged co-ions with moderate mobility, e.g. phthalic acid, pyridine-2,6-dicarboxylic acid, DL-phenylsuccinic acid, phenylphosphoric acid and SSA, only SSA shows an overall good separation for the standard ion mixture. Singly-charged co-ions, e.g. nitric acid and salicylic acid, have little effect on the separation. However, they do not bring about the desired separation for the selected ion mixture shown in Fig. 1.

With the decrease of the co-ion concentration, under the same pH, the concentration of the counter-ion decreases too. As a consequence, on the one hand, the cation effect (the interaction between the cations and the analytes) increases because the co-ion concentration is decreased. On the other hand, the cation effect decreases because the counter-ion concentration is decreased. However, as we found, the latter is stronger, leading to a faster mobility for multiply charged anions, e.g. a better separation of the pairs of e.g. $S_2O_3^{2-}$ / Br^-, SO_4^{2-} /NO_2^-, tartarate/ F^- as can be seen from the comparison of Fig. 1A and Fig. 3B.

A buffer with multiple visualizing ions or co-ions should be avoided to prevent the formation of detrimental system peaks [13]. The mobility of a system peak is located in between that of each of the adjacent two co-ions and closer to that of the co-ion with the smaller concentration. The SSA–Tris buffer contains, besides the co-ion SS, two other co-ions which are undesired. One is bromide which is

Table 1
Effective mobilities of some anions under the conditions in Fig. 1.

No.	Ions	Effective mobility ($m^2\ s^{-1}\ V^{-1}\ 10^{-9}$)	
		By el. inj.[a]	By hydr. inj.[b]
1	Thiosulfate	78.392	77.634
2	Bromide	76.498	75.502
3	Iodide	74.963	–
4	Chloride	74.622	73.887
5	Sulfate	72.117	71.503
6	Nitrite	70.980	70.508
7	Nitrate	69.720	69.026
8	Oxalate	68.494	67.789
9	Perchlorate	65.565	65.002
10	Thiocyanate	64.543	63.903
11	Sulfite	62.594	62.947
12	Citrate	61.124	60.500
13	Malate	57.153	56.922
14	Tartarate	55.767	55.453
15	Fluoride	54.954	54.533
16	Formate	54.140	53.651
17	HPO_4^{2-}	51.968	52.150
18	HCO_3^-	44.685	44.685
19	Acetate	40.291	40.194
20	Propionate	35.218	35.354
21	Trichloroacetate	-	34.526
22	Butyrate	31.783	32.001
23	Valerate	29.545	29.901

[a] Electrokinetic injection.
[b] Hydrostatic injection.

introduced with the surfactant HDB and the other is hydrogencarbonate, HCO_3^-, which is another form of CO_2 dissolved in the deionized water. Although the system peaks caused by the two co-ions are not significant (visible) due to their low concentrations, they are close to the peaks of bromide and hydrogencarbonate. As a consequence, the transfer ratio of bromide in a sample is affected, resulting in a much smaller bromide peak compared to chloride, and the HCO_3^- peak is deformed to an extent depending on the content of CO_2 in the buffer. Therefore, it is suggested that freshly prepared water should be used for making a buffer and it should be prevented from coming into contact with air.

With the exception of the rate of EOF, the temperature has little influence on the separation between 20 and 40°C.

3.3. EOF

When the EOF reversing reagent is set, the rate of the EOF is mainly influenced by the type of anions in the buffer. As shown in Fig. 3, the EOF rate is 31, 10 and 47 ($10^{-9}\ m^2\ s^{-1}\ V^{-1}$) when using chromate, 5-sulfosalicylate and salicylate as a visualizing ion, respectively. Obviously, the singly charged salicylate has the smallest effect and 5-sulfosalicylate the largest on the rate of EOF. When using a standard buffer with 3 m*M* SSA and a capillary which has not been coated with any surfactant, the reversed EOF rate increases roughly linearly to ca. 14–20 ($10^{-9}\ m^2\ s^{-1}\ V^{-1}$) with an increase in the concentration of HDB in the buffer to 0.0005%. Above 0.001% the change is small. Once the capillary is coated with HDB, the EOF rate changes a little by just flushing with buffer. The EOF of the capillary can be restored by flushing the capillary first with sodium dodecyl sulfate (SDS) (a strong interaction exists between these two surfactants with a different charge sign) and then 1 *M* NaOH.

3.4. Limit of detection (LOD)

The LODs of common ions are listed in Table 2. The corresponding electropherograms and those of deionized water are shown in Fig. 2. The factors which influence the LOD, such as the noise level of the baseline, the transfer ratio, the molar extinction coefficient of the visualizing ion and the injection method, will be discussed below.

3.4.1. Noise

Noise in indirect detection is composed of instrument noise and non-instrument noise [21]. The former is inherent to the optical system of the detector. It can be found by measuring the peak to peak noise of the baseline recorded during capillary flushing with the buffer at zero voltage. This noise is related to the energy of the incident light, the alignment of the light to the capillary window and the capillary dimensions. With a 50 μm I.D.×375 μm O.D. capillary and optimized detector conditions, the instrument noise is ca. 50 μAU.

Non-instrument noise consists of high and low frequency noise and/or disturbances and/or wavy baseline. It results from the concentration change or the absorbance change of the visualizing ion during electrophoresis with indirect detection. The concentration change is caused by the Joule heat produced in the capillary. A smaller heating effect and there-

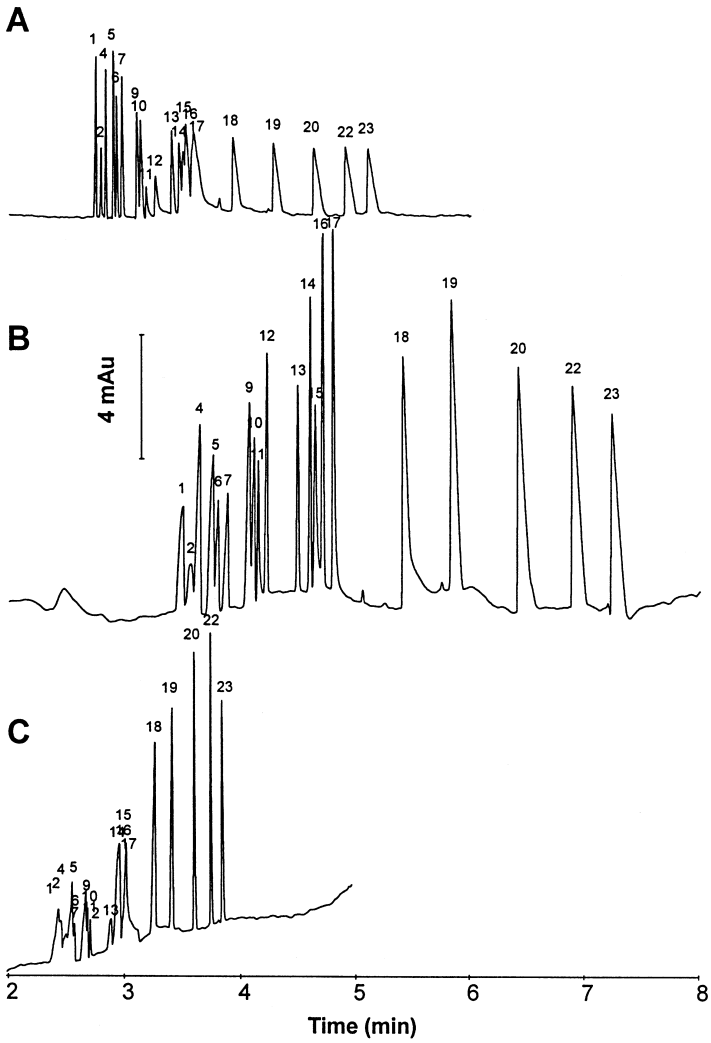

Fig. 3. Separation of some common anions with indirect detection using: (A) chromate, (B) 5-sulfosalicylate and (C) salicylate as visualizing ions. Conditions: separation solutions, (A) 5 m*M* chromium(VI), NH_3, pH 8.9, (B) 5 m*M* 5-sulfosalicylic acid, Tris, pH 8.2 and (C) 10 m*M* salicylic acid, Tris, pH 8.2. Separation: −30 kV/14.5 μA (A and C)/4.6 μA (B), 30°C; flushing between each run, with the running buffer containing 0.001% of HDB; Injection, −2 kV/22 s; indirect detection, 375, 210 and 220 nm for A, B and C, respectively (the large high frequency noise due to the old lamp in this comparison was filtered by a smoothing program); EOF rate, see text. Peaks and concentration refer to Fig. 1.

fore lower noise level and more stable baseline can be achieved by using a narrower capillary, a lower buffer concentration and a better cooling system [22,23]. Under the present conditions of 50 μm I.D. capillary/3 m*M* SSA buffer (−30 kV/5 μA) and a liquid forced cooling system, this noise is negligible. With the same conditions but with a 5 m*M* SSA buffer, an unstable baseline was observed, as shown in Fig. 3B. The same phenomenon is also observed in Fig. 3C. A stable baseline is expected when using a lower concentration of salicylate in the buffer.

3.4.2. Transfer ratio and molar absorptivity

From the transfer ratio point of view, a singly-charged visualizing ion is preferred. However the doubly charged visualizing ion SS has to be used for reasons of separation as discussed above. Fortunately, SS shows a high molar absorptivity. As can be

Table 2
Limit of detection (LOD) obtained by electrokinetic and hydrostatic injections

No.	Ions (ionic mass)	n*M*, ppb in injection solution		LOD (n*M*, ppb)	
		Electrokinetic inj. (Fig. 2A,a)	Hydrostatic inj. (Fig. 2B,a)	Electrokinetic inj.	Hydrostatic inj.
1	Thiosulfate (90)	25, 2.25	625, 56	8.0, 0.72	500, 45
2	Bromide (80)	25, 2.0	625, 50	10, 0.80	630, 50
3	Iodide (118)[a]	–	–	4.0, 0.47	260, 31
4	Chloride (36)	25, 0.90	625, 23	4.0, 0.14	260, 9
5	Sulfate (96.7)	15, 1.45	375, 61	2.2, 0.13	150, 15
6	Nitrite (46)	50, 2.3	1250, 58	12, 0.55	1100, 51
7	Nitrate (62)	50, 3.1	1250, 78	13, 0.80	860, 53
8	Oxalate (106)	25, 2.65	625, 66	4.5, 0.48	480, 51
9	Perchlorate (100)	50, 5.0	1250, 125	8.06, 0.81	590, 59
10	Thiocyanate (58)	50, 2.9	1250, 73	11.3, 0.66	960, 56
11	Sulfite (80)	25, 2.0	625, 50	8.6, 0.69	210, 17
12	Citrate (192)	25, 4.8	625, 120	37.3, 7.16	390, 75
13	Malate (114)	25, 2,85	625, 71	5.1, 0.58	360, 41
14	Tartarate (148)	25, 3.7	625, 93	6.6, 0.98	280, 41
15	Fluoride (19)	50, 0.95	1250, 24	12.5, 0.24	810, 15
16	Formate (45)	50, 2.25	1250, 56	5.6, 0.25	380, 17
17	HPO_4^{2-} (95)	50, 4.75	1250, 56	6.6, 0.63	390, 37
18	HCO_3^- (60)[b]	17000, 1020	17000, 1020	–	1370, 82
19	Acetate (59)	100, 5.9	2500, 148	9.3, 0.55	470, 28
20	Propionate (73)	100, 7.3	2500, 91	10.8, 0.79	830, 61
21	Trichloroacetate (162.5)	–	–	–	–
22	Butyrate (87)	100, 8.7	2500, 109	12.2, 1.06	530, 46
23	Valerate (102)	100, 10.2	2500, 128	12.8, 1.31	550, 56

Conditions see Fig. 2A,a (electrokinetic inj.) and Fig. 2B,a (hydrostatic inj.).
[a] Not present in Fig. 2.
[b] Present in the deionized water used for the dilution of injection solutions.

seen in Fig. 2, the peak intensity obtained by the SSA buffer is ca. four times larger than that of the doubly charged chromate buffer and two times larger than that of the singly charged salicylate buffer.

3.4.3. Injection modes

3.4.3.1. (a) Electrokinetic injection

Due to the low conductivity of the injection solution, the injection voltage must be kept low (−2 kV in this method) in this injection mode to avoid overheating of the injection plug. Therefore, the injection solution and the ions introduced to the capillary by the EOF is insignificant because the EOF rate is very small at this voltage. However, ions migrate to the capillary fast because almost all the voltage over the capillary is exerted to the injection solution with low conductivity. The injected amount of the ions depends on the conductivity of the injection solution and the mobility of the ions. With the stacking effect, very low LODs are achieved for a sample with extremely low conductivity as shown in Fig. 2. The LODs are around 5 and 10 n*M* for high and low mobility ions, respectively (Table 2). The dependence of the injection amount on the conductivity (sometimes pH for weak ions) of the injection solution makes the quantitative analysis often difficult. The maximum injection time at −2 kV, without significant change of peak shape and resolution with the concentrations shown in Fig. 1A, is found to be 22 s.

Normally the content of CO_2 in deionized water is found to be 5 to 30 μ*M*, depending on the time that it is exposed to the air. It is almost a thousand times higher than the concentration of the other ions in the case of Fig. 2A,b.

3.4.3.2. (b) Hydrostatic injection

In this injection mode the injection amount is only dependent on the injection plug length. The maximum injection time, at the concentrations shown in Fig. 1B, at 70 mbar (0.5 p.s.i.) without significant change of peak shape and resolution is found to be 66 s. However, the migration time of peaks increases significantly with the injection plug length. This is due to the fact that the EOF rate in the plug is much lower or may even be reversed. In addition, the long injection plug may cause a current break when the conductivity of the plug is low. Therefore, a long injection plug should normally be avoided. The injection time using this mode is limited to 30 s or less. The LODs obtained by this injection mode (Table 2) are almost two orders higher than those obtained by electrokinetic injection.

3.5. Calibrations

3.5.1. With electrokinetic injection

A standard ion mixture with the same ions and concentrations as described in Fig. 1 was diluted into a series of injection solutions. The upper limits of linearity of the peak areas found with these solutions are 0.5 μ*M* and 3 μ*M* for multiply- and singly-charged ions, respectively. Above those limits the peak areas of the ions change a little with the ion concentration, because the stacking effect decreases with an increase of the sample concentration (conductivity). When the concentrations of other ions in the injection solution are very low, the conductivity of the injection solution is dominated by carbon dioxide in the form of HCO_3^- and an approximately constant conductivity or stacking effect is obtained. Therefore, the amount of an ion injected or the peak area will linearly be related to the concentration of the ion in the injection solution. One paper [20] found that the linear range of the ions with mobility higher than that of HCO_3^- is 0.05–0.5 μ*M*, which is comparable with our findings.

If only one ion in the mixture is to be quantitated and this ion does not dominate the conductivity of the solution, a single ion addition method may be used. For instance, in the mixture as shown in Fig. 1, trichloroacetate (No. 21 in Table 1) is added and the change of the conductivity of the solution is considered negligible. The linearity of the calibration curve of trichloroacetate is extended to 30 μ*M* with $r^2 = 0.9994$. One must, however, bear in mind that the LOD, the linear range and the linear coefficient are dependent on the conductivity level of the injection solution. A higher conductivity results in a higher LOD (a smaller stacking effect), a wider linear range and a smaller linear coefficient. For instance, The LOD of trichloroacetate is ca. 10 n*M* when the conductivity of the injection solution approaches zero and ca. 500 n*M* (80 ppb) in the case as described above.

3.5.2. With hydrostatic injection

With this injection mode the amount of an ion injected is in most cases independent on sample properties, such as a conductivity. The upper limits of linearity of the peak area are found to be much higher than those with the electrokinetic injection mode. The linear range of singly charged ions is generally wider than that of multiply charged ions. This is probably due to the interaction of the latter with the capillary wall or the EOF modifier HDB. Quantitation with this injection method is believed to be more reliable than with electrokinetic injection and is suggested for routine analysis.

The statistic data and linear ranges of these calibration curves are listed in Table 3.

3.6. Identification

Because the EOF rate is dependent on the capillary wall condition, it changes slightly from day to day and from capillary to capillary. The absolute migration time is not applicable for the identification of ions. However, the mobilities of ions do not change if the electrophoretic conditions are fixed. Since HCO_3^- is almost always present in a sample solution and is easily recognized, it is convenient to calculate the effective mobilities of ions by taking the migration time or apparent mobility of HCO_3^- and its mobility as a reference. The calculation is carried out as follows:

An apparent mobility of an ion i, $\mu_{\text{apparent, i}}$ is measured by the migration time of the peak,

$$\mu_{\text{apparent, i}} = \left(\frac{L_{\text{eff}}}{t}\right) \Big/ E \qquad (1)$$

Table 3
Statistic regression results of the calibration curves when using a hydrostatic injection mode. $y(\text{area}) = ax(\mu M) + b$

Ions (ionic mass)	a	b	r^2	n	Linear up to (μM)
Oxalate (106)	223.2	−132	0.995	6	20
Citrate (192)	389.1	−307.7	0.9972	5	15
Malate (114)	217.4	129.6	0.993	7	25
Tartarate (148)	277	−86.7	0.998	7	25
Formate (45)	161.4	0 (force 0)	0.951	7	50
HCO_3^- (60)	176.2	−262.02	0.9998	6	200
Acetate (59)	224.9	710	0.9989	7	100
Propionate (73)	197.5	−369.2	0.9944	4	100
Butyrate (87)	296.13	312.2	0.9998	7	100
Valerate (102)	312.1	406.2	0.9998	7	100

where L_{eff} is the capillary length in meters to the detector, t the migration time of the peak in seconds and E the electric field strength in V m^{-1} over the capillary.

The effective or ionic mobility of the ion i, $\mu_{\text{effective, i}}$, is then written as,

$$\mu_{\text{effective, i}} = \mu_{\text{apparent, i}} - \mu_{\text{EOF}} \quad (2)$$

where μ_{EOF} is the mobility of the EOF.

In particular, the apparent and effective mobility of HCO_3^- can be expressed as,

$$\mu_{\text{effective, HCO}_3^-} = \mu_{\text{apparent, HCO}_3^-} - \mu_{\text{EOF}} \quad (3)$$

Combine Eqs. (2) and (3), we have,

$$\mu_{\text{effective, i}} = (\mu_{\text{apparent, i}} - \mu_{\text{apparent, HCO}_3^-}) + \mu_{\text{effective, HCO}_3^-} \quad (4)$$

Now, the values of all the terms on the right side of the Eq. (4) are known and hence the effective mobility may be calculated.

Because, in capillary zone electrophoresis (CZE), especially with indirect detection, overloading is inevitable, the way to measure the migration time of peaks is different from other column separation techniques. That is to say, the migration time is not always taken from the top of a peak. When a peak is overloaded the migration time is measured at the foot of the ramp side of the peak [14].

The effective mobility of some common ions is determined by taking the migration time and mobility of the HCO_3^- peak as a reference for both injection modes. As seen from Table 1, the effective mobilities obtained by the two injection modes differs slightly for the ions with high mobility.

3.7. Reproducibility and quantitation

Reproducibility and quantitation measurements were performed for some organic ions and carbonate, because they are normally not analyzed by IC in our laboratory.

The reproducibility of the migration time is excellent for all ions with the relative standard deviation (RSD) being less than 0.1% and 0.27% for electrokinetic injection and hydrostatic injection, respectively. The reproducibility of the peak area is also good with the RSD generally being less than 4% for both injection modes.

In a recovery experiment, ions to be recovered were added to a standard mixture with all other ions and concentrations shown in Fig. 1. The recovery lies in the range from 97.2 to 107.6% with a RSD less than 3.6% (Table 4). The content of carbon dioxide in deionized water which has been in contact with air for ca. 20 min is found to be 17 μM in this experiment.

3.8. Trace analysis

When using electrokinetic injection for trace analysis (ionic concentration less than 50 nM or less than a few ppb), e.g. a quality control of the ultra pure water, contamination is a non-negligible problem. One of the easily overlooked contamination sources is the rubber cap of the buffer and sample vials. This cap contains both inorganic and organic ions.

Table 4
Recovery and reproducibility of peak area of some organic ions and hydrogencarbonate with six successive hydrostatic injections (70 mbar or 0.5 psi/22 s).

Ions	Added[a] (μM)	Peak area			Found μM	Recovery %
		Mean	SD	RSD(%)		
Citrate	7.5	2531	108	4.3	7.30±0.27	97.3±3.6
Malate	7.5	1715	50	2.9	7.29±0.23	97.2±3.1
Tartarate	7.5	2135	76	3.5	7.66±0.29	102.1±2.1
Formate	15	2497	75	3.0	15.47±0.47	103.1±3.1
HCO_3^-	0	2764	51	1.8	17.00±0.45	–
Acetate	30	7683	197	2.6	31.00±0.88	103.3±3.3
Propionate	30	6010	181	3.0	32.3±0.9	107.6±3.0
Butyrate	30	9581	179	1.9	31.3±0.6	104.3±2.0
Valerate	30	10222	114	1.1	31.45±0.36	104.8±1.2

[a] Added to a mixture as shown in Fig. 1.

The sample volume should be as large as possible. It is found that the ion peaks decrease rapidly with successive injections from the same micro-injection-vial with a sample volume of 50 μl when the sample concentration is down to ppb level. This is due to the strong enrichment (stacking) effect at low (almost zero) conductivity of the sample solution, resulting in a gradual depletion of the ions in the sample.

4. Applications

Four forensic environmental samples have been analyzed with the method developed in this work. The results shown in Fig. 4 were compared with those obtained by IC in the following aspects.

4.1. Separation range

In general, the main advantage of CZE over IC is the separation of a wide range of ions in a short time with a single injection. With the current method, almost all inorganic and multiply-charged low-molecular-mass organic anions and all singly-charged organic acids with a mobility larger than $26 \cdot 10^{-9}$ m^2 s^{-1} V^{-1} (equivalent to heptanoic acid) will appear within 7.5 min, while this range of ions has to be separated with different columns in IC. Some ions show difficulty in separation or detection in IC but are analyzed without problem with CZE, e.g. SO_3^{2-} and HCO_3^-. For instance, the major components in Fig. 4A (unidentified, $\mu = 54.269$) and Fig. 4B (HCO_3^-) and some other ions (particularly organic ones) were missed by IC with the commonly used column for anion screenings but found by CZE.

4.2. Identification

The separation of ions in CZE is based on their mobility. At the pH used in this work (8.6), most low-molecular-mass acids are fully deprotonated so that the effective mobility measured is close to their ionic mobility. Therefore, for the ions which fall outside the standard ion mixture used in the current method, we can compare the ionic mobilities with those found in the literature [24]. Although the data published in the literature is often for infinitely diluted aqueous solutions and therefore somewhat different from those normally encountered, they give a limited range of ions for further investigation.

The separation of ions, however, in IC is based on the charge interaction between the ions and ion-exchange resin (except the ion-exclusion chromatography). The separation selectivity is quite different from that of CZE. This offers us an opportunity to identify uncertain peaks. The complementation of the two techniques strengthens the identification of ions.

4.3. Tolerance to sample metrics

It seems that CZE has better tolerance to sample metrics than IC, which was also found in a previously published paper [25]. For instance, sulfate can be

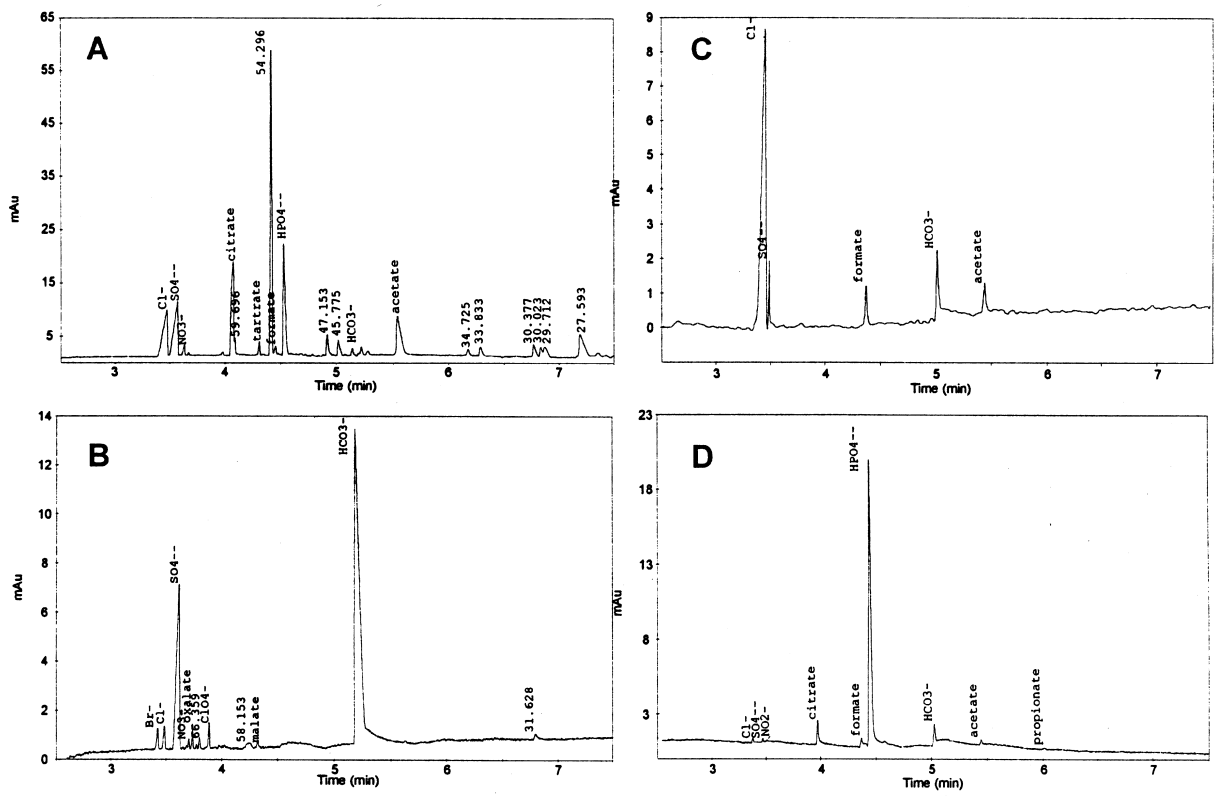

Fig. 4. Electropherograms of four forensic environmental samples. Dilution factor from A to D: 100, 100, 80 000, 4000. Other conditions are as in Fig. 1B.

easily determined when chloride is present in a large quantity, as shown in Fig. 4C.

5. Conclusion

The CZE method developed for the screening of low-molecular-mass ions in this work has a high separation efficiency and speed, a broad separation range, a very low limit of detection, a good reproducibility of mobilities and peak area, a good tolerance to sample matrices and a low cost of consumables. A good separation both for high and low mobility ions is achieved with a co-ion with a moderate mobility. In comparison to IC this method has a wider separation range with a single injection, a better tolerance to sample matrices and it is very suitable to be used for low-molecular-mass-ion screening. Due to the large difference in the separation selectivity of the CZE and IC techniques, they are complementary for the identification of ions present in the sample.

References

[1] S. Hjertén, Chromatogr. Rev. 9 (1967) 122.
[2] F.E.P. Mikkiers, F.M. Everaerts, Th.P.E.M. Verheggen, J. Chromatogr. 169 (1979) 11.
[3] J.W. Jorgenson, K.D. Lukacs, Anal. Chem. 53 (1981) 1298.
[4] J.W. Jorgenson, K.D. Lukacs, J. High Resolut. Chromatogr. Chromatogr. Commun. 4 (1981) 230.
[5] J.W. Jorgenson, K.D. Lukacs, Clin. Chem. 27 (1981) 1551.
[6] J. W Jorgenson, K.D. Lukacs, J. Chromatogr. 218 (1981) 208.
[7] S. Hjertén, K. Elenbring, F. Kilar, J.L. Liao, A.J.C. Chen, C.J. Siebert, M.D. Zhu, J. Chromatogr. 403 (1987) 47.
[8] F. Foret, S. Fanali, L. Ossicini, P. Boecek, J. Chromatogr. 470 (1989) 299.

[9] G.J.M. Bruin, A.C. van Asten, X. Xu, H. Poppe, J. Chromatogr. 608 (1992) 97.
[10] W.G. Kuhr, E.S. Yeung, Anal. Chem. 60 (1988) 1832.
[11] P.E. Andersson, W.D. Pfeffer, L.G. Blomberg, J. Chromatogr. A 699 (1995) 323.
[12] T.M. Olefirowicz, A.G. Ewing, J. Chromatogr. 499 (1990) 713.
[13] H. Poppe, Anal. Chem. 64 (1992) 1908.
[14] X. Xu, W.Th. Kok, H. Poppe, J. Chromatogr. A 742 (1996) 211.
[15] T. Wang, R.A. Hartwick, J. Chromatogr. 589 (1992) 307.
[16] J. Bullock, J. Strasters, J. Snider, Anal. Chem. 67 (1995) 3246–3252.
[17] P. Jandik, W.R. Jones, A. Weston, P.R. Brown, LC·GC 9 (1991) 634.
[18] W.R. Jones, in J.P. Landers (Editor), Handbook of Capillary Electrophoresis, CRC Press, Boca Raton, FL, 1994, Ch. 9.
[19] S. Motellier, K. Gurdale, H. Pitsch, J. Chromatogr. A 770 (1997) 311–319.
[20] Th. Ehmann, K. Bächmann, L. Fabry, H. Rüfer, S. Pahlke, L. Kotz, Chromatographia 45 (1997) 301–311.
[21] X. Xu, W.Th. Kok, H. Poppe, J. Chromatogr. A 786 (1997) 333–345.
[22] X. Xu, W.Th. Kok, H. Poppe, J. Chromatogr. A 716 (1995) 231.
[23] H. Poppe, X. Xu, in M.G. Khaled (Editor), High Performance Capillary Electrophoresis, Wiley, New York, 1998.
[24] T. Hirokawa, M. Nishino, N. Aoki, Y. Kiso, Y. Sawamoto, T. Yagi, J.-I. Akiyama, J. Chromatogr. 271 (1983) D1–D106.
[25] P.R. Haddad, J. Chromatogr. A 770 (1997) 281–290.